Supporting information for "Chemical and Electrochemical Hydrogenation of CO_2 to hydrocarbons on Cu Single Crystal Surfaces: Insights into the Mechanism and Selectivity from DFT Calculations"

Lihui Ou*

College of Chemistry and Chemical Engineering, Hunan University of Arts and Science, Changde 415000, China.

1. Mathematical details about electrochemical environment [1]

In this technique, zero voltage is defined based on the reversible hydrogen electrode (RHE), in which the reaction

$$H^+ + e^- \leftrightarrow \frac{1}{2}H_2$$

is defined to be in equilibrium at zero voltage, at all values of pH, at all temperatures, and with H_2 at 101325 Pa pressure. Therefore, in the CHE, the chemical potential of a proton-electron pair, $\mu(H^+)+\mu(e^-)$ is equal to half of the chemical potential of gaseous hydrogen ($\frac{1}{2}\mu(H_2)$) at a potential of 0 V. In this way, the chemical potential of proton-electron pair can be calculated simply by calculating the chemical potential of gas-phase H_2. The chemical potential of the proton-electron pair can be adjusted as a function of the applied potential by the standard relation between chemical and electrode potential, $\Delta G = -eE$, where e is the elementary positive charge and E is the applied bias. Since the RHE is defined to be at 0 V at all pH values, a pH correction is not needed. Thus, the total chemical potential of the proton-electron pair as a function of applied potential, at all temperature and pH values, can be calculated as

$$\mu(H^+)+\mu(e^-)=\frac{1}{2}\mu(H_{2(g)})-eE$$

As an example, to calculate the free energy change from adsorbed CH_2 to adsorbed CH_3, the free energy change of the below chemical reaction needs to be calculated:

$$CH_2* + (H^+ + e^-) \rightarrow CH_3*$$

Where an asterisk (*) indicates that the species is adsorbed on the copper surface. The free energy change of this reaction would thus be:

$$\Delta G = \mu(CH_3*) - \mu(CH_2*) - [\mu(H^+) + \mu(e^-)]$$
$$= \mu(CH_3*) - \mu(CH_2*) - [\frac{1}{2}\mu(H_{2(g)}) - eE]$$

Thus, the CHE model allows the potential (E) to be explicitly contained within the free energy change of each step.

Table S1. Adsorption energies and geometrical structure of CO_2 and H_2 molecules on the Cu(111) and Cu(100) surfaces

Crystal Face	Adsorption State	E_{ad}(eV)	$R_{C(H)\text{-}O(H)}$(Å)	$\theta_{O\text{-}C(H)\text{-}O}$(°)	$R_{C(O)\text{-}Cu(111)}$(Å)
Cu(111)	CO_2-Phys.	-0.00680	1.172	179.9819	3.793
	H_2-Phys.	-0.00272	0.753	/	3.530
Cu(100)	CO_2-Phys.	-0.0136	1.172	179.8459	3.620
	CO_2-Chem.	0.3808	1.336	126.6454	1.586
	H_2-Phys.	-0.0054	0.753	/	3.482
	H_2-Chem.	0.0612	0.784	/	1.893

Table S2. Adsorption energies and geometrical structure of possible products CH_4, C_2H_4, HCOO, COOH on the Cu(111) and Cu(100) Surfaces

Crystal Face	Adsorption State	Adsorption Site	E_{ad}(eV)	$R_{adsorbates\text{-}Cu(111)}$(Å)
Cu(111)	CH_4	Hcp	-0.02	3.813
	C_2H_4	Top	-2.78	2.202
	HCOO	Bridge	-2.79	1.992
	Cis-COOH	Bridge	-1.51	1.971
	Trans-COOH	Bridge	-1.56	1.834
Cu(100)	CH_4	4-fold hollow	-0.09	3.856
	C_2H_4	Top	-2.87	2.250
	HCOO	Bridge	-3.03	2.010

	Cis-COOH	4-fold hollow	-1.70	2.139
	Trans-COOH	4-fold hollow	-1.74	2.129

2. Reaction intermediates of CO_2 reduction on the Cu(111) Surface

Fig. S1 shows the preferential adsorption configurations for various intermediates and products on the Cu(111) surface. The corresponding adsorption energies are listed in Table S3. CO adsorption is isoenergetic on both the fcc and hcp sites with C-end toward the surface. Experimentally, chemisorbed CO is mostly found on the top sites of Cu surface,[2-6] while in DFT calculations the fcc-hollow site is energetically most favorable. The discrepancy between the theory and experiment is caused by the overestimation of the back-donation into the $2\pi^*$ orbital of CO which is mainly due to the fact that the HOMO-LUMO gap is too small in most of the DFT exchange-correction functional. In this case, the $2\pi^*$ orbital interacts stronger with the surface electrons at the hollow site than at the top site.[7]

CHO adsorbs through C and O atoms on a bride site, while COH prefers fcc and hcp hollow sites. CH_2O and CHOH adsorb through C and O atoms to hollow sites. Other possible hydrocarbons such as C, CH, CH_2, CH_3 prefers fcc hollow sites adsorption through C atom.

Carboxyl (COOH) exhibits two stable structures on the Cu(111) surface: (1) one with the O-H bond pointing away from the surface (cis-COOH) and (2) one with the O-H bond pointing toward the surface (trans-COOH). The trans-COOH species is about 0.05 eV more stable than the cis-COOH. The most stable configuration of the adsorbed formate is the bidentate (bridge) HCOO. Ethylene (C_2H_4) adsorbs through two C atoms to a top site; the adsorption energy is -2.78 eV. These results were listed in Table S2.

Various co-adsorbed structures of intermediates on the Cu(111) surface, including (CO+O)*, (CO+OH)*, (H+OH)*, (H+H)*, (O+H)*, (CO+H)*, (CHO+H)*, (CH+O)*, (C+OH)*, (CH_2+O)*, (C+H)*, (CH+H)*, (CH_2+H)*, (CH_3+H)*, (CH_2+CH_2)* are shown in Fig. S2. The co-adsorption energies of some co-adsorbed structures are less negative than the sum of the adsorption energy of the individual adsorbates, such as (CO+O)*, (CO+OH)*, (H+OH)*, (O+H)*, (CO+H)*, (CHO+H)*, (CH_2+H)*, (CH_2+CH_2)*, indicating the repulsive interaction of the co-adsorbed surface species. The corresponding adsorption energies are

listed in Table S4.

Table S3. Adsorption energies and preferential sites of possible reaction Intermediates on the Cu(111) Surface

Species	Adsorption Site	E_{ad}(eV)
CO	Fcc	-0.83
	Hcp	-0.83
O	Fcc	-4.87
	Hcp	-4.79
H	Fcc	-2.49
	Hcp	-2.49
	Top	-1.86
OH	Fcc	-3.20
	Hcp	-3.16
CHO	Bridge	-1.26
	Hcp	-1.25
CH_2O	Fcc	-1.26
	Bridge	-0.018
	Hcp	-0.026
	Fcc	-0.030
COH	Fcc	-2.67
	Hcp	-2.63
CHOH	Fcc	-2.53
	Hcp	-2.55
C	Fcc	-4.67
	Hcp	-4.62
	Top	-2.78
CH	Fcc	-4.85
	Hcp	-4.80
CH_2	Fcc	-2.93

CH_3	Hcp	-2.91
	Fcc	-1.39
	Hcp	-1.40

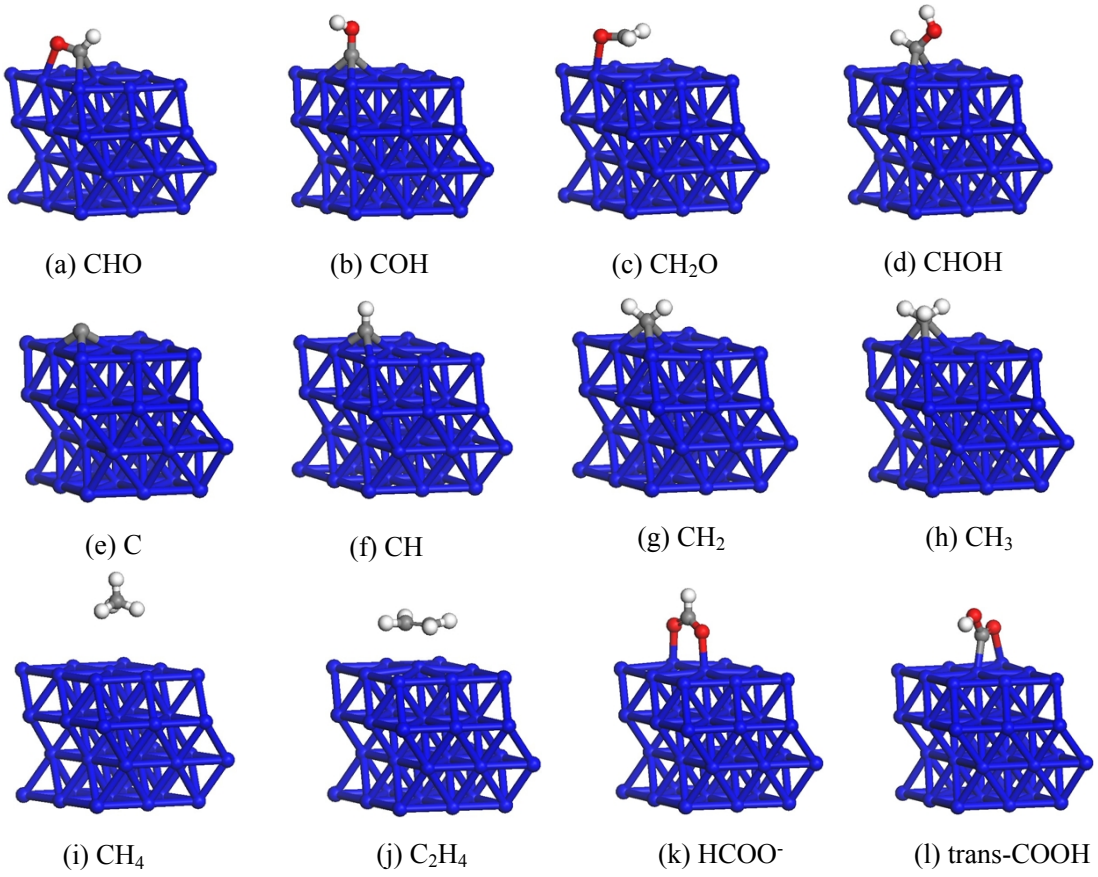

Fig. S1. The preferential adsorption configurations of the most stable adsorption state of reaction intermediates and products of CO_2 reduction on the Cu(111) surface.

Table S4. Adsorption energies of the most stable structure of co-adsorbed intermediates ($E_{co\text{-}ad}$, eV) on the Cu(111) surface, compared with the sum of the separated adsorption (E_{ad}, eV)

Species	$E_{co\text{-}ad}$	E_{ad}	ΔE_{ad}(eV)
CO(hcp) + O(fcc)	-5.58	-5.70	0.12
CO(hcp) + OH(fcc)	-3.97	-4.03	0.06
H (hcp)+ OH(fcc)	-5.66	-5.69	0.03
H(hcp) + H(fcc)	-5.01	-4.98	-0.03
CO(fcc) + H(hcp)	-3.31	-3.32	0.01

CHO(fcc)+H(hcp)	-3.71	-3.75	0.04
CH_2(hcp)+O(fcc)	-1.86	-1.80	-0.06
CH(hcp) + O(fcc)	-9.79	-9.72	-0.07
C(hcp) + OH(fcc)	-8.06	-7.87	-0.19
O(fcc) + H(hcp)	-7.30	-7.36	0.06
C(hcp) + H(fcc)	-7.17	-7.16	-0.01
CH(hcp) + H(hcp)	-7.36	-7.34	-0.02
CH_2(fcc) + H(hcp)	-5.39	-5.42	0.03
CH_3(hcp) + H(fcc)	-3.88	-3.88	0.00
CH_2(hcp) + CH_2(hcp)	-2.77	-2.78	0.01

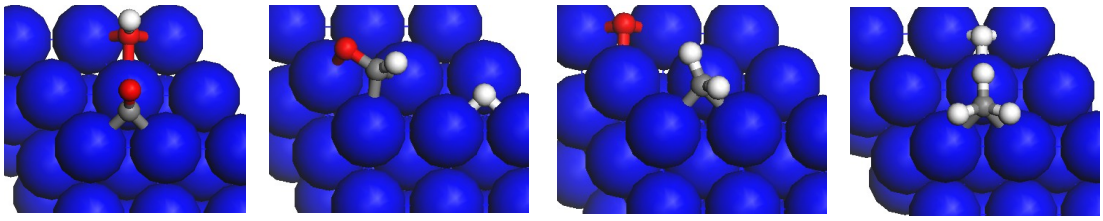

(a) CO + OH (b) CHO + H (c) CH_2 + O (d) CH_3 + H

Fig. S2. Geometrical structures of the most stable co-adsorption site of partial reaction intermediates of CO_2 reduction on the Cu(111) surface.

3. Reaction intermediates of CO_2 reduction on the Cu(100) Surface

Fig. S3 shows the preferential adsorption configurations for various intermediates on the Cu(100) surface. The corresponding adsorption energies are listed in Table S5. For atomic hydrogen adsorption at various sites on the Cu(100) surface, the 4-fold hollow site was found to be the most stable site. Atomic oxygen also shows a clear preference for the 4-fold hollow site, the bridge and top sites were found to be unstable sites. They do not correspond to an energy local minimum, and O goes to 4-fold hollow site during the geometry optimization. For OH adsorption at various sites on the Cu(100) surface. The top site was found to be an unstable site. It does not correspond to an energy local minimum, and OH goes to the 4-fold hollow site during the geometry optimization, with its axis perpendicular to the surface. As starting points for the formation of CH_x species, the adsorption nature of CO on the Cu(100)

surface is examined, the chemisorption of CO on the Cu(100) surface follows the stability order 4-fold hollow > bridge > top. CO adsorbs at these sites perpendicular to the surface with the C-end toward the surface. CO on the Cu(100) surface at coverage of 1/9 monolayer (ML) preferentially occupies the 4-fold hollow site with an adsorption energy as strong as -0.88 eV, which agrees well with other theoretical calculations at a similar level of theory.[2-6] CHO attaches to the surface via C and O atoms occupying the 4-fold hollow sites, and the COH attaches to the surface via C atom occupying the 4-fold hollow sites, The most stable adsorption sites of C and CH on the Cu(100) surface are the 4-fold hollow site. For CH_2 adsorption at various sites on the Cu(100) surface, the bridge and top sites were found to be unstable sites, they does not correspond to an energy local minimum, and CH_2 goes to the 4-fold hollow site during the geometry optimization. For CH_3, the bridge site was found to be the most stable site. The order of adsorption energies of CH_x on the Cu(100) surface follows the trends: C > CH > CH_2 > CH_3. An analysis of the best binding configurations found in this study indicates that adsorbates on the Cu(100) surface appear to follow gas-phase coordination and bond order trends. As increasing H atom coordinated to C atom, the effective coordination number of C to Cu(100) surface is lowered, thus weaking C-Cu interaction.[8] The CH_2O and CHOH that obtained via CHO hydrogenation attach to the surface via C and O atoms occupying the 4-fold hollow sites, respectively. Similar to that on the Cu(111) surface, the co-adsorbed states of the intermediates were also computed prior to search the transition states of CO_2 reduction on the Cu(100) surface. The sum of the adsorption energies of the most stable structure were listed in Table S6.

The adsorption sites and adsorption energies of four possible products on the Cu(100) surface were listed in Table S2. The trans-COOH species is ca. 0.04 eV thermodynamically more stable than the cis-COOH. Adsorbed formate ($HCOO^-$) shows that the most stable configuration is bidentate (bridge) HCOO. The adsorption energy of the most stable configuration of C_2H_4 on the Cu(100) surface is -2.87 eV.

Table S5. Adsorption energies and preferential sites of possible reaction intermediates on the Cu(100) surface

Species	Adsorption Site	E_{ad}(eV)
CO	Bridge	-0.82
	4-fold hollow	-0.88
	Top	-0.77
O	Bridge	-5.42
	4-fold hollow	-5.42
	Top	-5.42
H	Bridge	-2.32
	4-fold hollow	-2.48
	Top	-1.72
OH	Bridge	-3.30
	4-fold hollow	-3.47
	Top	-3.47
CHO	Bridge	-1.39
	4-fold hollow	-1.50
	Top	-1.18
CH_2O	Bridge	-0.19
	4-fold hollow	-0.52
	Top	-0.10
COH	Bridge	-2.41
	4-fold hollow	-3.07
	Top(Bridge)	-2.41
CHOH	4-fold hollow	-2.66
	Top	-2.33
C	Bridge	-4.06
	4-fold hollow	-6.06
	Top	-2.85
CH	Bridge	-4.27
	4-fold hollow	-5.61

	Top	-3.14
CH_2	4-fold hollow	-3.20
CH_3	bridge	-1.41

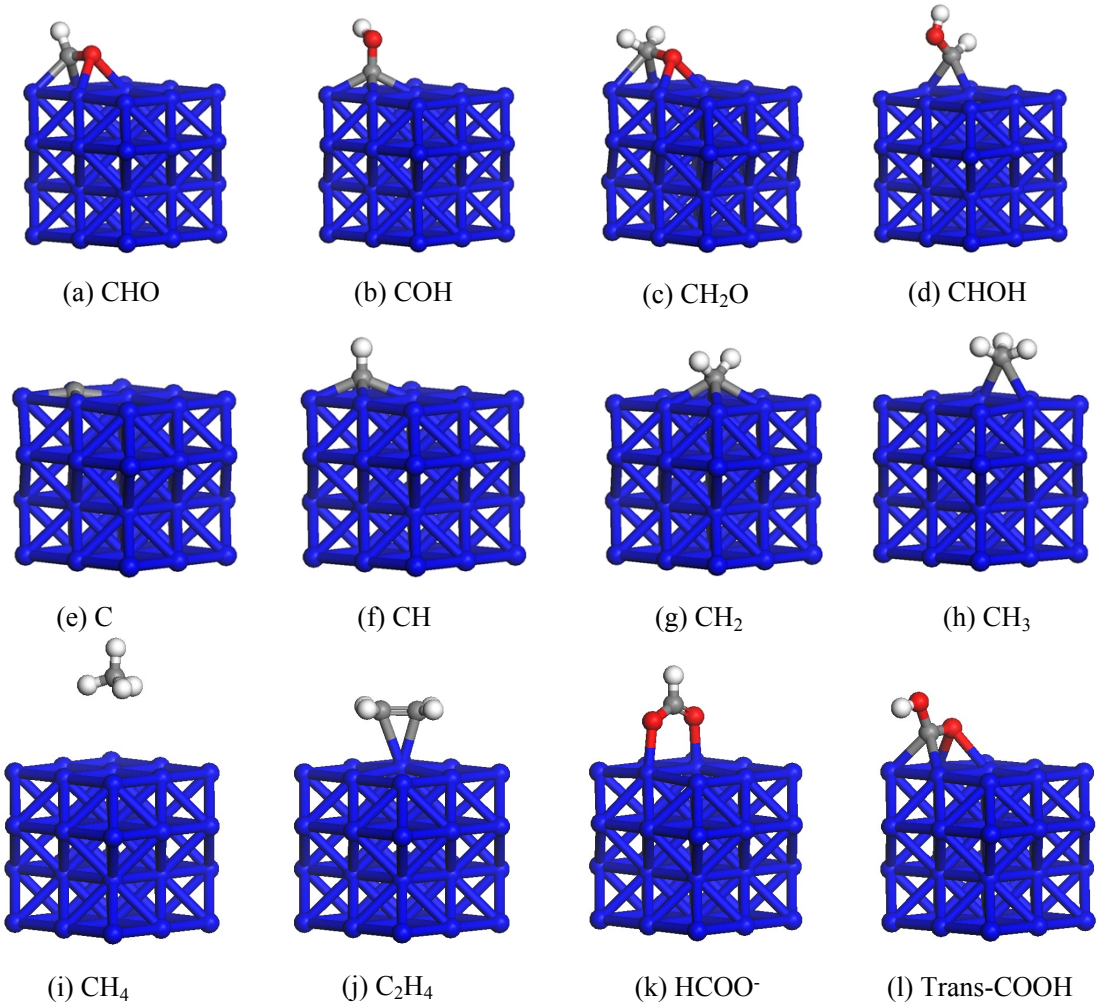

Fig. S3. The preferential adsorption configurations of the most stable adsorption state of reaction intermediates and products of CO_2 reduction on Cu(100) surface.

Table S6. Adsorption energies of the most stable structure of co-adsorbed intermediates ($E_{co\text{-}ad}$, eV) on the Cu(100) surface, compared with the sum of the separated adsorption (E_{ad}, eV)

Species	$E_{co\text{-}ad}$	E_{ad}	ΔE_{ad}(eV)
CO_2(bridge)+H(hollow)	-2.50	-2.49	-0.01
CO(bridge) + O(hollow)	-6.30	-6.30	0.00
CO(bridge) + OH(hollow)	-4.32	-4.35	0.03

C(hollow) + O(hollow)	-10.87	-11.48	0.61
H(hollow) + OH(hollow)	-5.85	-5.95	0.10
H(hollow) + H(hollow)	-4.96	-4.96	0.00
CO(bridge) + H(hollow)	-3.35	-3.36	0.01
CH(hollow) + O(hollow)	-10.45	-11.03	0.58
C(hollow) + OH(bridge)	-9.22	-9.53	0.31
O(hollow) + H(bridge)	-7.75	-7.90	0.15
C(hollow) + H(hollow)	-8.36	-8.54	0.18
CH(hollow) + H(hollow)	-7.87	-8.09	0.22
CHO(hollow) + H(hollow)	-3.92	-3.98	0.06
CH_2(hollow) + CH_2(hollow)	-5.87	-6.40	0.53
CH_2(hollow) + O(hollow)	-8.02	-8.62	0.60
CH_2(hollow)+H(hollow)	-5.49	-5.68	0.19
CH_3(hollow)+H(hollow)	-3.88	-3.89	0.01

References

1 J. K. Nørskov, J. Rossmeisl, A. Logadottir and L. Lindqvist, *J. Phys. Chem. B*, 2004, **108**, 17886-17892.

2 P. Hollins and Pritchard, J, *Surf. Sci*., 1979, **89**, 486-495.

3 W. Kirstein, B. Krüger and F. Thieme, *Surf. Sci*., 1986, **176**, 505-529.

4 I. Bönicke, W. Kirstein, S. Spinzig and F. Thieme, *Surf. Sci*., 1994, **313**, 231-238.

5 S. Kneitz, J. Gemeinhardt and H. P. Steinrück, *Surf. Sci*., 1999, **440**, 307-320.

6 P. J. Feibelman, B. Hammer, J. K. Nørskov, F. Wagner, M. Scheffler, R. Stumpf, R. Watwe and J. Dumesic, *J. Phys. Chem. B*, 2001, **105**, 4018-4025.

7 A. Gil, A. Clotet, J. M. Ricart, G. Kresse, M. García-Hernández, N. Rösch and P. Sautet, *Surf. Sci*., 2003, **530**, 71-87.

8 J. Greeley and M. Mavrikakis, *J. Am. Chem. Soc*., 2002, **124**, 7193-7201.